

## Optical diffusion imaging using a direct inversion method

C. P. Gonatas

*Exxon Research and Engineering Company, Annandale, New Jersey 08801  
and Departments of Biochemistry and Biophysics, Radiology, and Physics,  
University of Pennsylvania, Philadelphia, Pennsylvania 19104*

Masaru Ishii, John S. Leigh, and John C. Schotland

*Department of Radiology, University of Pennsylvania, Philadelphia, Pennsylvania 19104*

(Received 16 February 1994; revised manuscript received 4 May 1995)

We image the spatial structure of an optically inhomogeneous absorbing medium using multiply scattered light in the diffusive limit. We infer structure by using a solution of the inverse scattering problem that is valid to first order in the optical absorption. These results on imaging with diffusive light extend recent work on light scattering probes of colloids, foams, and biological tissues.

PACS number(s): 42.25.Fx, 42.68.Ay

### I. INTRODUCTION

A small amount of the light incident on a seemingly opaque object such as a colloid, a slab of concrete, or a person may travel a great distance within the object instead of being absorbed or reflected at the initial point of incidence. This scattered light senses physical processes that are not easily probed with conventional techniques such as x-ray tomography or confocal microscopy. Thus the study of multiply scattered light has led to tools for the investigation of colloids, foams, and biological tissues [1]. In this paper we extend these methods by using multiply scattered light to image spatial structure within an object.

Internal scattering centers quickly randomize the direction of a photon traveling within an object. The motion of scattering centers causes random phase shifts observable in the intensity autocorrelation function. By summing millions of independent laser pulses and time averaging the speckle pattern, we may neglect effects due to the photon phase. If the size of the system greatly exceeds the transport mean free path  $l^*$ , then photons propagate diffusively such that the photon energy density becomes analogous to the temperature in a thermally conducting solid [2].

Delpy *et al.* [3] and Patterson *et al.* [4] pioneered the measurement of optical constants in homogeneous media using time-resolved measurements of scattered light. In the long-time limit Beer's law,  $T = \exp(-\mu_a s)$ , governs the optical transmission  $T$  where  $\mu_a$  is the absorption coefficient and  $s$  is the photon pathlength. The asymptotic slope of  $\ln T$  for large optical pathlengths enables the measurement of the absorption coefficient for an unbounded homogeneous medium. If  $l^*$  is spatially uniform then it can also be accurately determined [5, 6]. For a bounded heterogeneous medium this simple analysis fails [7] because it is necessary to weight each subregion with the local photon transmission probability. Here we demonstrate the surprising result that the pattern of scattered light diffused through a heterogeneous ob-

ject can be used to infer the spatial structure embedded within.

Interestingly, Beer's law also applies for time-resolved imaging experiments in the short-time limit [8, 9]. In these experiments, time-gated detectors select only the very earliest arriving, "ballistic" photons thereby forming a projection image. Ballistic photons undergo very few scattering events and thus  $T$  reflects the line of sight absorption. The number of ballistic photons, however, falls exponentially with increasing sample size (the image degrades if later time, multiply scattered photons are collected) thus necessitating a more powerful laser. This, unfortunately, may not always be suitable for biological samples. Consequently, a method utilizing the much greater number of diffusive photons would be advantageous.

### II. THEORY

The transport of diffusive photons in a system with a spatially varying optical absorption  $\mu_a(r)$  is governed by

$$\frac{\partial u(r, t)}{\partial t} = D \nabla^2 u(r, t) - \alpha(r) u(r, t) + S(r, t), \quad (1)$$

where  $u(r, t)$  is the energy density,  $\alpha(r) = c\mu_a(r)$ ,  $S(r, t)$  is the source power density, and  $D = \frac{1}{3}(c/n)l^*$  is the photon diffusion coefficient. In this work, we assume that the diffusion coefficient is spatially uniform. We denote by  $\delta\alpha(r)$  the spatial fluctuation in the absorption which is defined by  $\delta\alpha(r) = \alpha(r) - \alpha_0$ , where  $\alpha_0$  is the background absorption. We further define the transmission as  $T = u/u_0$ , where  $u_0$  is the energy density of transmitted photons in a reference system with absorption  $\alpha_0$ . Although the actual observable is the photon flux rather than the energy density, the two are simply related [5, 10, 11]. For a pulse of photons emanating from a point source the energy density is determined by the diffusion propagator for (1). The propagator may be obtained from a perturbative expansion [12] in  $\delta\alpha(r)$  which to lowest

order is of the form

$$G(r_1, r_2; t) = G_0(r_1, r_2; t) + \int d^3r \int_0^t dt' G_0(r_1, r; t') \times \delta\alpha(r) G_0(r, r_2; t - t'), \quad (2)$$

where  $G_0(r_1, r_2; t)$  is the propagator evaluated in the absence of spatial fluctuations in the absorption. In an infinite medium  $G_0(r_1, r_2; t)$  is given by

$$G_0(r_1, r_2; t) = \frac{1}{(4\pi Dt)^{\frac{3}{2}}} \exp\left(-\frac{(r_1 - r_2)^2}{4Dt} - \alpha_0 t\right). \quad (3)$$

We consider an experiment in which an optical pulse propagates from a point source at  $r_1$  and is detected at  $r_2$  at time  $t$ . In this situation an integral equation for the transmission,  $T(r_1, r_2, t)$ , may be obtained from (2) and is of the form

$$T(r_1, r_2, t) = 1 - \int d^3r \nu(r; r_1, r_2, t) \delta\alpha(r), \quad (4)$$

where the fluctuation in the Beer's law absorption coefficient is weighted by the kernel

$$\nu(r; r_1, r_2, t) = \frac{1}{G_0(r_1, r_2; t)} \times \int_0^t dt' G_0(r_1, r; t') G_0(r, r_2; t - t'). \quad (5)$$

Several comments on this result are necessary. First, we are considering only *single* scattering of the energy density  $u(r, t)$  by  $\delta\alpha(r)$  even though the photons themselves are multiply scattered. Second, in this approximation (4) is valid in the limit of weak fluctuations in the optical absorption. In the case of strong absorption note that (4) is still valid provided that the fluctuation term  $\delta\alpha(r)$  is sufficiently small [13]. Finally, the kernel  $\nu(r; r_1, r_2, t)$  may be interpreted as the conditional probability distribution of a photon that passed through  $r$  assuming that it traversed a path beginning at  $r_1$  and was detected at  $r_2$  at time  $t$  [14, 15]. See Fig. 1. Calculations of  $\nu(r; r_1, r_2, t)$  for selected geometries are reported elsewhere [15].

Equation (4) provides the solution to the forward scattering problem. In an alternative approach, Singer *et al.*

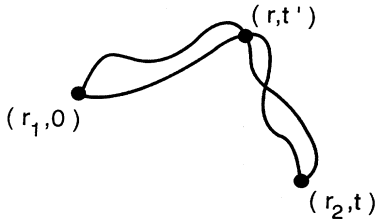


FIG. 1. Photon paths that begin at the source position  $(r_1, 0)$ , end at the detector position  $(r_2, t)$ , and pass through the point  $r$  at time  $t'$ . In this treatment, the photons may be absorbed *only* at the point  $r$ .

[16] and Arridge *et al.* [17] use Monte Carlo simulations to solve the forward problem. They then solve the inverse problem iteratively. We avoid iteration by using a *direct* inversion of the integral equation (4). In order to accomplish this (4) is discretized and converted into a system of linear algebraic equations that relate measurements of the transmission to the absorption in specific volume elements of the sample. Assuming an experimental configuration with  $P$  sources,  $Q$  detectors, and  $M$  time points (4) becomes

$$T_{ijk} = 1 - \int_{\Omega} d^3r \nu_{ijk}(r) \delta\alpha(r), \quad (6)$$

where  $T_{ijk}$  and  $\nu_{ijk}(r)$  denote  $T(r_1, r_2, t)$  and  $\nu(r; r_1, r_2, t)$  evaluated at the  $i$ th source position,  $j$ th detector position, and  $k$ th time point and  $\Omega$  denotes the sample. We discretize  $\nu_{ijk}(r)$  and  $\delta\alpha(r)$  by decomposing  $\Omega$  into  $N$  elements of volume  $\Delta V$  by assuming that  $\nu_{ijk}(r)$  and  $\delta\alpha(r)$  are constant in each volume element, giving

$$\sum_{l=1}^N A_{ijk}^l a_l = b_{ijk}, \quad (7)$$

where  $A_{ijk}^l = \nu_{ijk}(r_l) \Delta V$ ,  $a_l = \delta\alpha(r_l)$ ,  $b_{ijk} = 1 - T_{ijk}$ , and  $r_l$  denotes the center of the  $l$ th volume element. Note that (7) gives  $PQM$  equations for the transmission in terms of the  $N$  unknown absorptions. If we regard  $A_{ijk}^l$  as a  $PQM \times N$  matrix then we can use standard numerical methods employing singular value decomposition [18, 19] to obtain the solution of (7) in the form

$$a_l = \sum_{i,j,k} (A^+)_{ijk}^l b_{ijk}, \quad (8)$$

where  $A^+$  denotes the Tikhonov-regularized pseudoinverse of  $A$ . In practice we overdetermine (8) so that the regularization method tapers the smallest singular values, thereby reducing numerical instability.

### III. EXPERIMENT

The above procedure gives the internal structure of the object [in the form of  $\mu_a(r)$ ] in terms of the observable  $T(r_1, r_2, t)$  and the kernel  $\nu(r; r_1, r_2, t)$ . Thus obtaining the spatial structure from observed quantities is feasible and we can use this analysis in an imaging experiment. In our apparatus, illustrated by the inset in Fig. 2, we introduce a light pulse into a scattering medium and detect the transmitted intensity in a time-resolved measurement. A typical plot of photon intensity versus time is depicted in Fig. 2.

The experimental apparatus we use has been previously described [5]. Briefly, we introduce laser pulses (50 ps wide at 780 nm) into a 20 cm  $\times$  20 cm  $\times$  40 cm chamber containing a milky-white scattering suspension (Intralipid). The "object" to be imaged consists of one or more tubes containing Intralipid of the same concentration as the ambient bath, together with a small quantity of ink. A fiber collects scattered light from multiple po-

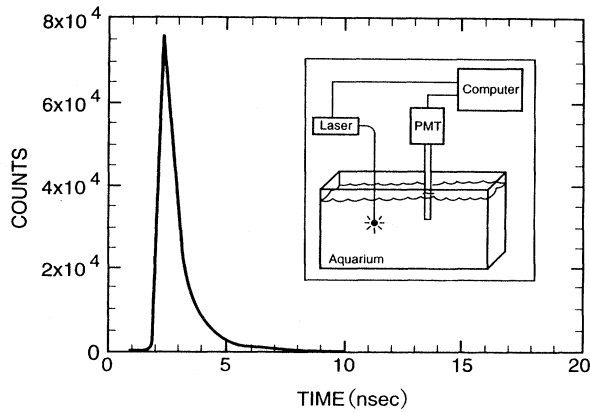


FIG. 2. A typical plot of intensity as a function of time after the beginning of a laser pulse. (Inset: diagram of apparatus.)

sitions in the bath and guides it into a photomultiplier. We denote by  $S(t)$  the measured flux of scattered light. The optical fiber guiding the light to the detector is inclined by  $90^\circ$  relative to the source-detector axis. For this inclination angle, the photon flux is proportional to the photon energy density [10].

To calculate the kernel  $\nu(r; r_1, r_2, t)$  we first measure  $l^*$  and determine  $D$  [5]. For different source-detector locations we measure the transmission  $T(t) = S(t)/S_0(t)$ , where  $S_0(t)$  is the transmitted flux in the absence of an absorber. Although measuring  $S_0(t)$  for a biological object could present practical difficulties,  $S_0(t)$  may be calculated instead, given  $l^*$  and the absolute detector sensitivity.

In Fig. 3 we show an experimentally determined  $7 \times 11$

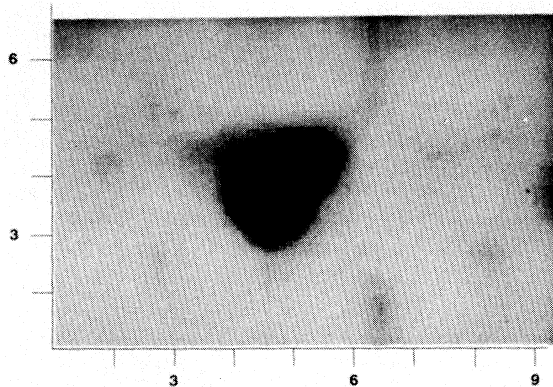


FIG. 3. Reconstruction of a  $7 \times 11$  cm<sup>2</sup> field of view. Dark tones correspond to greater optical absorption. The object is a 1.4 cm diameter tube containing  $5 \mu\text{l}$  ink, together with Intralipid and is shown in cross section. The actual location of the test tube is at the center of the field of view, corresponding to the reconstructed position.

cm cross section of  $\mu_a(r)$  for an Intralipid bath ( $l^* = 0.3$  mm) containing a 1.4 cm diameter tube. The tube, aligned along the  $\hat{z}$  axis, is characterized by an absorption  $\mu_a = 0.64$  cm<sup>-1</sup>. The experimentally determined value for the absorption is  $\mu_a(\text{object}) = 0.34$  cm<sup>-1</sup>, or a factor of 2 below the true absorption. The true location of the tube, near the reconstructed position, is at the center of the field.

We obtained the image shown in Fig. 3 using a source and detector separated by a fixed distance of 5 cm in the  $\hat{x}$  direction, while scanning the object in the  $\hat{x}$  and  $\hat{y}$  directions. We used a total of 13 independent displacements and divided each light pulse into 10 independent time segments resulting in 130 time-position points. We also used the symmetry of the object to infer data at three separate  $\hat{z}$  positions and at four separate  $45^\circ$  rotations about the axis of the tube.

In Fig. 4(a) we show a 3.2 cm square cross section of the measured  $\mu_a(r)$  for an Intralipid bath ( $l^* = 0.5$  mm) containing three equally spaced tubes of 5.5 mm

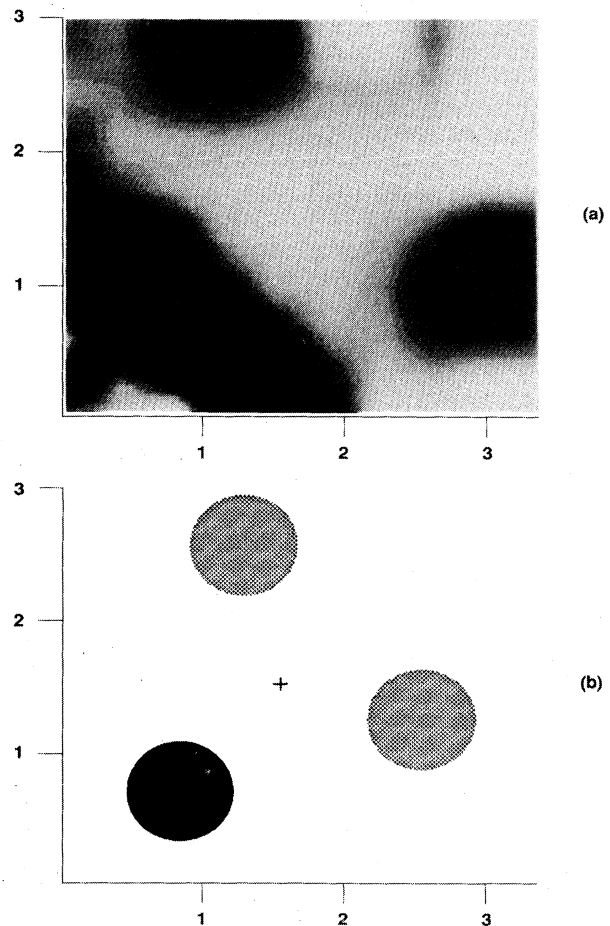


FIG. 4. Reconstruction of a 3.2 cm square field (a) containing the object depicted in (b). Dark tones correspond to greater optical absorption. The bottom left tube contains twice the ink concentration of the other tubes.

diameter. Figure 4(b) shows their true positions. The top and right tubes have absorption  $\mu_a = 0.13 \text{ cm}^{-1}$ . The bottom left tube has absorption  $\mu_a = 0.2 \text{ cm}^{-1}$ . The measured absorptions are  $\mu_a = 0.15 \text{ cm}^{-1}$  and  $\mu_a = 0.24 \text{ cm}^{-1}$ , respectively.

In the second data set the source and detector are separated by 6 cm in the  $\hat{x}$  direction, while the object is scanned  $\pm 8$  mm in the  $\hat{y}$  direction. At each scan position, we rotated the object through  $135^\circ$  in  $45^\circ$  steps to obtain an additional factor of 4 independent measurements. Data at three separate  $\hat{z}$  positions are inferred. We divide each light pulse into ten independent bins and exclude all early arrival time photons.

As with the object imaged in Fig. 3, we profit from symmetry to reduce the amount of data we require. Thus we could perform our experiment using only a two-dimensional translation stage and a rotator to position the object. The symmetry of the object is exact and the time-resolved transmissions are reproducible, so our use of symmetry would not appear to preclude the generality of the method to image more complicated objects.

The second set of absorption measurements agrees quantitatively with the actual absorption, although the reconstruction of the first data set differs by a factor of 2. This discrepancy can be explained by the violation of the weak-absorption limit under which (4) holds. Nonetheless, the location of the absorber in Fig. 3 was reconstructed accurately.

#### IV. DISCUSSION

The above analysis treats only time-resolved data but with modifications it is readily adapted for a continuous wave (cw) source. In a cw experiment photon diffusion is time independent and the equation governing the energy density becomes

$$D\nabla^2 u(r) - \alpha(r)u(r) + S(r) = 0. \quad (9)$$

As before an integral equation for the optical transmission may be derived and is of the form

$$T(r_1, r_2) = 1 - \int d^3r \nu(r; r_1, r_2) \delta\alpha(r), \quad (10)$$

where

$$\nu(r; r_1, r_2) = \frac{1}{G_0(r_1, r_2)} G_0(r_1, r) G_0(r, r_2). \quad (11)$$

Here  $G_0(r_1, r_2)$  is the diffusion Green's function evaluated in the absence of spatial fluctuations in the absorption and is given by

$$G_0(r_1, r_2) = \frac{1}{4\pi D} \frac{e^{-k|r_1 - r_2|}}{|r_1 - r_2|}, \quad (12)$$

where  $k = (\alpha_0/D)^{1/2}$  is the wave number of the diffusing wave.

The cw experiment is appealing because of its simplicity and could be used in an inexpensive application with a dc source. We performed the time-resolved experiment because of the additional data acquired from multiple time points. We estimate that obtaining ten independent time points permits a reduction by a factor of 2–4 in the number of independent source-detector positions, depending on the geometry of the object.

In an amplitude-modulated cw experiment a diffusing wave is generated that can be measured [20, 21] with phase-sensitive detection of the transmitted light. A calculation along the lines discussed for the cw case yields an expression for the transmission similar to (10) with the wave number modified as  $k = [(\alpha_0 + i\omega)/D]^{1/2}$ , where  $\omega$  is the source modulation frequency. A particularly attractive form of the cw experiment would make use of an array of modulated sources that may be phased to null the background absorption. The cw technique obtains only a single phase-amplitude data point per source-detector configuration and may require additional source-detector pairs compared to the time-resolved case. However, encouraging recent experiments [22] suggest that the advantage of phase nulling may outweigh this potential drawback.

In conclusion, we introduce a technique for interpreting light scattering data in the presence of *inhomogeneous* optical absorption. This technique is more powerful than simple object location because we may reconstruct a continuous distribution of absorption. In the weak fluctuation limit the resultant maps of optical absorption are quantitative.

#### ACKNOWLEDGMENTS

We thank B. Chance and A. Yodh for their interest and encouragement. This work was supported by the University of Pennsylvania Research Foundation and the NIH.

[1] *Scattering and Localization of Classical Waves in Random Media*, edited by P. Sheng (World Scientific, Singapore, 1990).

[2] Because the angular dependence of light scattering may be anisotropic, the transport mean free path  $l^*$  appears in the diffusive transport equation. The transport mean free path  $l^* = l/(1 - g)$ , where  $g$  is the average cosine of the scattering angle and  $l$  is the mean free path. See A.

Ishimaru, *Wave Propagation and Scattering in Random Media* (Academic Press, San Diego, 1978), Vol. 1.

[3] D. Delpy, M. Cope, P. van der Zee, S. Arridge, S. Wray, and J. Wyatt, *J. Phys. Med. Biol.* **33**, 1422 (1988).

[4] M. Patterson, B. Chance, and B. Wilson, *Appl. Opt.* **28**, 2331 (1988).

[5] C. P. Gonatas, M. Miwa, M. Ishii, J. Schotland, B. Chance, and J. S. Leigh, *Phys. Rev. E* **48**, 2212 (1993).

- [6] P. D. Kaplan, M. H. Kao, and A. G. Yodh, *Appl. Opt.* **32**, 3828 (1993).
- [7] J. Haselgrove, J. Schotland, and J. Leigh, *Appl. Opt.* **31**, 2678 (1992).
- [8] K. M. Yoo, F. Liu, and R. R. Alfano, *Opt. Lett.* **16**, 1068 (1993); L. Wang, P. P. Ho, C. Liu, G. Zhang, and R. R. Alfano, *Science* **253**, 769 (1991).
- [9] D. A. Benaron and D. K. Stevenson, *Science* **259**, 1463 (1993).
- [10] To first order, the flux  $J$  crossing the plane of a detector perpendicular to  $\hat{n}$  is given in terms of the energy density  $u$  by  $J = \frac{c}{4}(u - \hat{n} \cdot \nabla u/h)$ , where  $h$  is a constant obtained from transport theory. The asymmetry in the flux reflects the fact that photon propagation is not isotropic. For an infinite medium the angular dependence of the flux simplifies so that for a detector perpendicular to the source the flux is proportional to the energy density.
- [11] F. Liu, K. Yoo, and R. Alfano, *Opt. Lett.* **18**, 432 (1993).
- [12] E. Economou, *Green's Functions in Quantum Physics* (Springer-Verlag, New York, 1983).
- [13] It is difficult to state precise conditions under which the perturbative expansion in the integral equation breaks down. Nevertheless, computer simulations reveal that even when fluctuations in the absorption are sufficiently large (to preclude quantitative reconstruction of the absorption) the spatial structure of the medium is reconstructed accurately.
- [14] J. Schotland and J. Leigh, *Biophys. J.* **61**, 446 (1992).
- [15] J. Schotland, J. Haselgrove, and J. Leigh, *Appl. Opt.* **32**, 448 (1993).
- [16] J. Singer, F. Grünbaum, P. Kohn, and J. Zubelli, *Science* **248**, 990 (1990).
- [17] S. R. Arridge, P. van der Zee, M. Cope, and D. T. Delpy, *SPIE Proc.* **1431**, 123 (1991).
- [18] E. J. Aymebellegarda, T. M. Habashy, and J. R. Belle-garda, *Opt. Eng.* **31**, 2572 (1992).
- [19] W. H. Press, S. Teukolsky, W. Vetterling, and B. Flannery, *Numerical Recipes in C* (Cambridge University Press, Cambridge, 1990).
- [20] J. Fishkin and E. Gratton, *J. Opt. Soc. Am. A* **10**, 127 (1993).
- [21] M. O'Leary, D. Boas, B. Chance, and A. Yodh, *Phys. Rev. Lett.* **69**, 2658 (1992); *Phys. Rev. E* **47**, R2999 (1993).
- [22] M. O'Leary, D. Boas, B. Chance, and A. Yodh, *Opt. Lett.* **20**, 426 (1995).

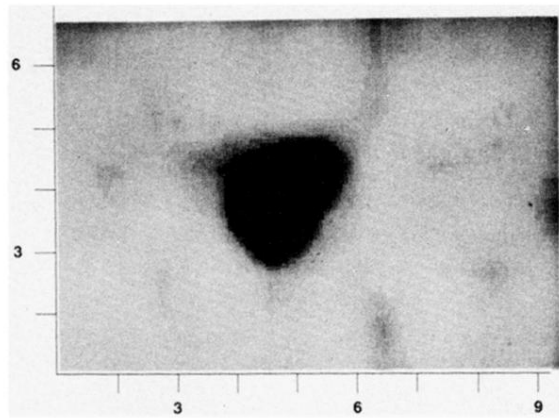


FIG. 3. Reconstruction of a  $7 \times 11 \text{ cm}^2$  field of view. Dark tones correspond to greater optical absorption. The object is a 1.4 cm diameter tube containing  $5 \mu\text{l}$  ink, together with Intralipid and is shown in cross section. The actual location of the test tube is at the center of the field of view, corresponding to the reconstructed position.

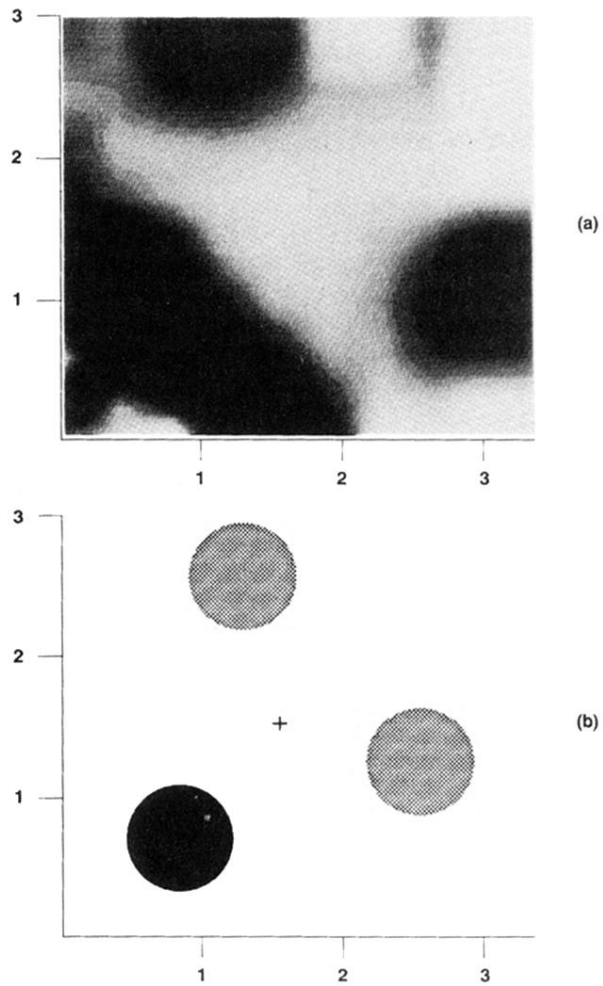


FIG. 4. Reconstruction of a 3.2 cm square field (a) containing the object depicted in (b). Dark tones correspond to greater optical absorption. The bottom left tube contains twice the ink concentration of the other tubes.